Research Article | Vol. 30, No. 16 / 1 Aug 2022 / Optics Express 28668
Optics EXPRESS

Circular dichroism in magneto-optical forces

SHULAMIT EDELSTEIN,[1] ANTONIO GARCIA-MARTIN,[2] PEDRO A. SERENA,[1] AND MANUEL I. MARQUÉS[3,*]

[1]*Instituto de Ciencia de Materiales de Madrid (ICMM-CSIC), Campus de Cantoblanco, 28049 Madrid, Spain*
[2]*Instituto de Micro y Nanotecnología IMN-CNM, CSIC, CEI UAM+CSIC, Isaac Newton 8, Tres Cantos, 28760 Madrid, Spain*
[3]*Departamento de Física de Materiales, IFIMAC and Instituto de Física de Materiales "Nicolás Cabrera" Universidad Autónoma de Madrid, 28049 Madrid, Spain*
[*]*manuel.marques@uam.es*

Abstract: In this article we use an exact method to resolve the fields scattered by a spherical magneto-optical particle and calculate the optical forces exerted on it. The resulting force and the contributing components, i.e. magneto-optical gradient force and magneto-optical extinction force, are presented in an analytical form. We also derive analytical expressions for the scattering and extinction cross sections of a magneto-optical particle, expressions which intuitively demonstrate the effect of circular dichroism in magneto-optical scattering and forces. Finally, we demonstrate that the magneto-optical extinction force is the result of circular dichroism in magneto-optical scattering. We show that it is possible to completely cancel the scattering in the forward or in the backward direction, when the incident field is composed of a circularly-polarized reflected beam. Moreover, the directional scattering is interrelated to the direction of the force exerted on the particle.

1. Introduction

Magneto-optical (MO) materials have become a key tool in functional nanophotonics. The unique nonreciprocal effect and magnetic tuneability of magneto-optical devices make them play an irreplaceable role in high-performance isolators, polarization controllers, modulators, and magnetic field sensors [1,2].

When an external magnetic field is applied, a magneto-optical particle exhibits an anisotropic behavior and its permittivity takes a tensor form. The analysis of wave propagation and scattering in magneto-optical medium becomes very difficult, as for this problem, Maxwell's equations are not separable in spherical coordinates.

The problem of scattering of an electromagnetic wave by a magneto-optical spherical particle was solved in the literature both analytically and numerically using various methods. Among them, a generalization of Mie scattering to the case where the dielectric constant is a tensor with axial symmetry [3], spectrum domain Fourier transform approach [4], a modification of the discrete dipole approximation (DDA) [5,6], the generalized Lorenz-Mie theory (GLMT) [7] and Extended Boundary Condition Method (EBCM) [8–10].

Interaction between an electromagnetic wave and a particle leads to mechanical actions on the particle, what is known as optical forces. Evaluation of optical forces requires knowledge of the scattered field and analytical expressions for optical forces on a single particle were derived using GLMT [11,12], the dipole approximation [13,14], generalized Mie theory [15] and more [16]. These expressions led to the classification of optical forces into gradient and scattering components. However, the expressions were derived for isotropic particles mainly.

In earlier papers, we used the dipole approximation to analyze optical forces on MO particles [17,18]. We found that the MO effect leads to an additional contribution to optical forces, a

#464252 https://doi.org/10.1364/OE.464252
Journal © 2022 Received 17 May 2022; revised 29 Jun 2022; accepted 7 Jul 2022; published 20 Jul 2022

Optics EXPRESS

contribution which can also be classified into gradient and extinction (scattering) components [17].

In this paper, we use the method of eigen-expansion of the field in terms of spherical vector wave functions (SVWF) and Fourier expansion for the unknown spectrum amplitude [19] to find an exact solution for the field scattered by a magneto-optical particle. We then apply the solution to the analysis of the optical forces exerted on such a particle, where we adapt analytical expressions previously developed for optical forces on isotropic particles [15] to the MO case.

Magnetic Circular Dichroism (MCD), the differential absorption of left-handed circularly polarized (LCP) light and right-handed circularly polarized (RCP) light in the presence of a magnetic field, arises from the magnetic field induced Zeeman interactions of electronic structure [20]. MCD spectroscopy is a predominant technique in studying excitonic transitions in semiconductor nanocrystals, electronic transitions in noble metal nanoclusters, and plasmon resonances in noble metal nanostructures. Moreover, MCD has provided new opportunities in exploring the relationship between structure and magneto-optical properties in nanomaterials [21].

The method we chose to solve the magneto-optical scattering problem [19], naturally reflects the inherent circular dichroism in the magneto-optical scattering process. The solution obtained for the scattered field is used to derive general expressions for the scattering and extinction cross sections and to evaluate scattering and extinction circular dichroism for magneto-optical particles. We show that circular dichorism constitutes a property of scattering interaction of electromagnetic twisted fields [22] and is not only an effect due to absorption.

We also show that MO forces can be further classified into the contributions from the electric and magnetic dipoles and an additional contribution from the interactions between the two, very much like an isotropic particle [23–25] but with the addition of circular dichroism.

Tailoring electromagnetic scattering based on subwavelength nanostructures has gained an unprecedented development attributed to the recent explosion in the number of investigations on metamaterials [26,27]. However, active control of directional scattering using a simple nanostructure still remains a challenging problem [28,29].

In the present paper, we show that when positioned in a standing-wave, a MO particle scattering direction can be controlled with the direction of an external magnetic field bias, enabling active control of directional scattering. The directional scattering leads to MO extinction force in a direction opposite to the scattering direction. An isotropic particle positioned in the same field will not experience any force at all.

The combination of mechanical action by optical forces and the active tuning of directional scattering are of interest for the design of state-of-the-art functional nanophotonic devices, nanoantennas engineering, sensors and enhancement of circular dichroism (CD, MCD) spectroscopies [21,30].

2. Electric and magnetic fields scattered from magneto-optical particle

Consider a magneto-optical particle of radius a positioned in free space. Assuming a monochromatic incident wave with time dependence $e^{-i\omega t}$, Maxwell's equations in such source-free magneto-optical medium can be written in the following form:

$$\begin{aligned} \nabla \times \mathbf{E} &= i\omega\mu_0 \mathbf{H}, \\ \nabla \times \mathbf{H} &= -i\omega\hat{\epsilon}\mathbf{E}, \end{aligned} \tag{1}$$

where $\mathbf{E}$ and $\mathbf{H}$ denote the electric and magnetic fields respectively, μ_0 is the free-space permeability and $\hat{\epsilon}$ is the permittivity tensor for the magneto-optical medium. If an external constant magnetic field $\mathbf{B}_{ext}$ is applied in the z-direction (parallel to the propagation direction of the incident wave, in the so-called "polar" configuration. See Fig. 1), the permittivity tensor $\hat{\epsilon}$

Optics EXPRESS

takes the following form:

$$\hat{\epsilon} = \epsilon_0 \begin{bmatrix} \epsilon_1 & -\epsilon_2 & 0 \\ \epsilon_2 & \epsilon_1 & 0 \\ 0 & 0 & \epsilon_3 \end{bmatrix}, \tag{2}$$

where the permittivity tensor elements ϵ_1, ϵ_2 and ϵ_3 are complex functions of ω, electron density, phonon frequency and the strength of the applied constant magnetic field. From Eq. (1), we can reach the electric field vector wave equation:

$$\nabla \times \nabla \times \mathbf{E} - \omega^2 \hat{\epsilon} \mu_0 \mathbf{E} = 0. \tag{3}$$

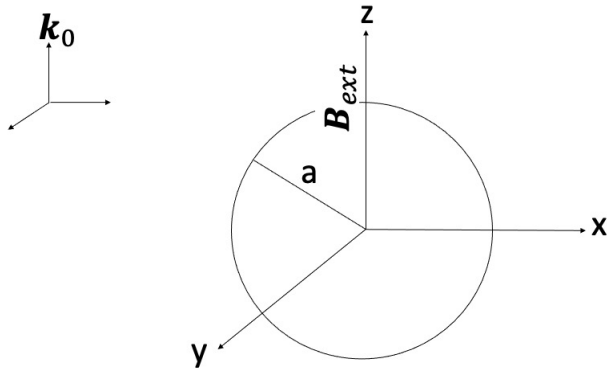

Fig. 1. The geometry considered in this paper. A magneto-optical spherical particle or radius a positioned in an electromagnetic field whose propagation direction $\mathbf{k}_0$ is parallel to the direction of an external constant magnetic field $\mathbf{B}_{ext}$.

Unlike scattering from an isotropic particle, in the magneto-optical case, we cannot reduce Eq. (3) to the simpler scalar wave equation (homogeneous Helmholtz equation). A plane wave which enters a magneto-optical media is decomposed into two circularly polarized waves propagating at different velocities and the value of the k vector, $\mathbf{k} = k_x\hat{x} + k_y\hat{y} + k_z\hat{z}$, is dependent on the direction. Hence, solutions to the vector wave equation must be found.

For that purpose, we expand the incident fields and the scattered fields in terms of spherical wave vectors $\mathbf{M}_{mn}^{(l)}$, $\mathbf{N}_{mn}^{(l)}$ and $\mathbf{L}_{mn}^{(l)}$ which form a complete set of vector basis functions [19,31] in spherical coordinate system (r, θ, ϕ).

$$\begin{aligned}
\mathbf{M}_{mn}^{(l)} =& z_n^{(l)}(kr)\left(im\frac{P_n^m(\cos\theta)}{\sin\theta}\hat{\theta} - \frac{dP_n^m(\cos\theta)}{d\theta}\hat{\phi}\right)e^{im\phi}, \\
\mathbf{N}_{mn}^{(l)} =& e^{im\phi}\left[n(n+1)\frac{z_n^{(l)}(kr)}{kr}P_n^m(\cos\theta)\hat{r} + \right. \\
& \left.\frac{1}{kr}\frac{d\left(rz_n^{(l)}(kr)\right)}{dr}\left(\frac{dP_n^m(\cos\theta)}{d\theta}\hat{\theta} + im\frac{P_n^m(\cos\theta)}{\sin\theta}\hat{\phi}\right)\right], \\
\mathbf{L}_{mn}^{(l)} =& \frac{kdz_n^{(l)}(kr)}{d(kr)}P_n^m(\cos\theta)e^{im\phi}\hat{r} + \\
& \frac{kz_n^{(l)}(kr)}{kr}\left(\frac{dP_n^m(\cos\theta)}{d\theta}\hat{\theta} + im\frac{P_n^m(\cos\theta)}{\sin\theta}\hat{\phi}\right)e^{im\phi},
\end{aligned} \tag{4}$$

Optics EXPRESS

where $z_n^{(l)}(kr)$ denotes the corresponding kind of spherical Bessel or Hankel function ($z_n^{(1)}(kr) = j_n(kr)$, $z_n^{(2)}(kr) = y_n(kr)$, $z_n^{(3)}(kr) = h_n^{(1)}(kr)$, $z_n^{(4)}(kr) = h_n^{(1)}(kr)$), P_n^m is the associated Legendre function and $\hat{r}$, $\hat{\theta}$ and $\hat{\phi}$ are the unit vectors in the radial, angular and azimuthal directions respectively.

Because spherical Bessel functions of the first to fourth kinds satisfy the same differential equation and the same recursive relations, the first kind of vector wave functions in Eq. (4) can be generalized to the second to fourth kinds.

Assuming that the electric field of the incident plane wave is given by $\mathbf{E}_{inc} = E_0\left(A_{0x}\hat{x} + A_{0y}\hat{y}\right)e^{i(\pm kz-\omega t)}$, the incident fields may be expanded in an infinite series of spherical vector wave functions as follows (The coefficients of $\mathbf{L}_{mn}^{(l)}$ are zero when the medium is isotropic [31])

$$\begin{aligned}\mathbf{E}_{inc} =& E_0\sum_{n=0}^{\infty}\sum_{m=\pm1}\left[\left(A_{0x}a_{mn}^{x} + A_{0y}a_{mn}^{y}\right)\mathbf{M}_{mn}^{(1)}(r,k_0) + \left(A_{0x}b_{mn}^{x} + A_{0y}b_{mn}^{y}\right)\mathbf{N}_{mn}^{(1)}(r,k_0)\right],\\ \mathbf{H}_{inc} =& \frac{E_0k_0}{i\omega\mu_0}\sum_{n=0}^{\infty}\sum_{m=\pm1}\left[\left(A_{0x}a_{mn}^{x} + A_{0y}a_{mn}^{y}\right)\mathbf{N}_{mn}^{(1)}(r,k_0) + \left(A_{0x}b_{mn}^{x} + A_{0y}b_{mn}^{y}\right)\mathbf{M}_{mn}^{(1)}(r,k_0)\right],\end{aligned} \tag{5}$$

where $k_0 = \omega/c$, and the coefficients of the incident fields are [31]

$$\begin{aligned} a_{1n}^{x} =& b_{1n}^{x} = E_n,\\ a_{-1n}^{x} =& n(n+1)E_n,\\ b_{-1n}^{x} =& -n(n+1)E_n,\\ a_{1n}^{y} =& b_{1n}^{y} = -iE_n,\\ a_{-1n}^{y} =& n(n+1)iE_n,\\ b_{-1n}^{y} =& -n(n+1)iE_n,\end{aligned} \tag{6}$$

for an incident beam propagating in the $+z$ direction, and

$$\begin{aligned} a_{1n}^{x} =& (-1)^n E_n,\\ b_{1n}^{x} =& (-1)^{n+1}E_n,\\ a_{-1n}^{x} =& b_{-1n}^{x} = n(n+1)(-1)^n E_n,\\ a_{1n}^{y} =& -i(-1)^n E_n,\\ b_{1n}^{y} =& i(-1)^n E_n,\\ a_{-1n}^{y} =& b_{-1n}^{y} = n(n+1)i(-1)^n E_n,\end{aligned} \tag{7}$$

for an incident beam propagating in the $-z$ direction. For both propagation directions, $E_n = i^{n+1}\frac{(2n+1)}{2n(n+1)}$.

According to the radiation condition of the scattered wave (attenuating to zero at infinity) and the asymptotic behavior of spherical Bessel functions, only $h_n^{(1)}$ satisfies this condition, therefore the expansion of the scattered fields in terms of spherical wave vectors is given by

$$\begin{aligned}\mathbf{E}_s =& E_0\sum_{n=0}^{\infty}\sum_{m=-n}^{n}\left[A_{mn}^{s}\mathbf{M}_{mn}^{(3)}(r,k_0) + B_{mn}^{s}\mathbf{N}_{mn}^{(3)}(r,k_0)\right],\\ \mathbf{H}_s =& \frac{E_0k_0}{i\omega\mu_0}\sum_{n=0}^{\infty}\sum_{m=-n}^{n}\left[A_{mn}^{s}\mathbf{N}_{mn}^{(3)}(r,k_0) + B_{mn}^{s}\mathbf{M}_{mn}^{(3)}(r,k_0)\right].\end{aligned} \tag{8}$$

The scattering coefficients are unknown and will be found from boundary conditions on the particle-medium interface. The fields inside the magneto-optical particle can be represented in

Optics EXPRESS

terms of the following eigenfunctions [19]

$$\begin{aligned}\mathbf{E}_{int} =&2\pi\sum_{q=1}^{2}\sum_{n=0}^{\infty}\sum_{m=-n}^{n}\sum_{n'=0}^{\infty}G_{mn'q}\int_0^{\pi}P_{n'}^{m}(\cos\theta_k)\sin\theta_k k_q^2\Big[A_{mnq}^{e}(\theta_k)\,\mathbf{M}_{mn}^{(1)}(r,\,k_q)+\\&B_{mnq}^{e}(\theta_k)\,\mathbf{N}_{mn}^{(1)}(r,\,k_q)+C_{mnq}^{e}(\theta_k)\,\mathbf{L}_{mn}^{(1)}(r,\,k_q)\Big]d\theta_k,\\ \mathbf{H}_{int} =&2\pi\sum_{q=1}^{2}\sum_{n=0}^{\infty}\sum_{m=-n}^{n}\sum_{n'=0}^{\infty}G_{mn'q}\int_0^{\pi}P_{n'}^{m}(\cos\theta_k)\sin\theta_k k_q^2\Big[A_{mnq}^{h}(\theta_k)\,\mathbf{M}_{mn}^{(1)}(r,k_q)+\\&B_{mnq}^{h}(\theta_k)\,\mathbf{N}_{mn}^{(1)}(r,\,k_q)+C_{mnq}^{h}(\theta_k)\,\mathbf{L}_{mn}^{(1)}(r,\,k_q)\Big]d\theta_k,\end{aligned}\tag{9}$$

where $G_{mn'q}$ is unknown, $A_{mnq}^{e}, B_{mnq}^{e}, C_{mnq}^{e}, A_{mnq}^{h}, B_{mnq}^{h}$ and C_{mnq}^{h} are given in Appendix A and $\theta_k = \tan^{-1}(\sqrt{k_x^2+k_y^2}/k_z)$. $k_{1,2}^2 = \frac{B\pm\sqrt{B^2-4AC}}{2A}$ is the root of the bi-quadratic equation $Ak_q^4 - Bk_q^2 + C = 0$ where

$$\begin{aligned}A =&a_1\sin^2\theta_k + a_3\cos^2\theta_k,\\ B =&\left(a_1^2+a_2^2\right)\sin^2\theta_k + a_1a_3\left(1+\cos^2\theta_k\right),\\ C =&a_3\left(a_1^2+a_2^2\right),\end{aligned}$$

and $a_j = \omega^2\epsilon_j\mu_0$.

We then use boundary conditions from the continuity of the tangential components of the electric and magnetic fields on the particle-medium interface, to reach two sets of linear equations

$$\begin{aligned}2\pi\sum_{q=1}^{2}\sum_{n'=0}^{\infty}G_{mn'q}Q_{mnq}^{n'} &= \frac{iE_0}{(k_0a)^2}\left(\delta_{m,\pm1}\right)a_{mn}^{p},\\ 2\pi\sum_{q=1}^{2}\sum_{n'=0}^{\infty}G_{mn'q}R_{mnq}^{n'} &= \frac{iE_0}{(k_0a)^2}\left(\delta_{m,\pm1}\right)b_{mn}^{p},\end{aligned}\tag{10}$$

where a_{mn}^{p} and b_{mn}^{p} (p=x,y) are the coefficients of the incident fields, given in Eq. (6) and

$$\begin{aligned}Q_{mnq}^{n'} =&\int_0^{\pi}\Big[A_{mnq}^{e}(\theta_k)\frac{1}{k_0r}\frac{d\left[rh_n^{(1)}(k_0r)\right]}{dr}j_n\left(k_qa\right)-\\&h_n^{(1)}(k_0a)\frac{i\omega\mu_0}{k_0}\Big(B_{mnq}^{h}(\theta_k)\frac{1}{k_qr}\frac{d\left[rj_n\left(k_qr\right)\right]}{dr}+\\&C_{mnq}^{h}(\theta_k)\frac{j_n\left(k_qr\right)}{r}\Big)\Big]_{r=a}P_{n'}^{m}(\cos\theta_k)\,k_q^2\sin\theta_k d\theta_k,\\ R_{mnq}^{n'} =&\int_0^{\pi}\Big[\frac{i\omega\mu_0}{k_0}A_{mnq}^{h}(\theta_k)\frac{1}{k_0r}\frac{d\left[rh_n^{(1)}(k_0r)\right]}{dr}j_n\left(k_qa\right)\\&-h_n^{(1)}(k_0a)\Big(B_{mnq}^{e}(\theta_k)\frac{1}{k_qr}\frac{d\left[rj_n\left(k_qr\right)\right]}{dr}+\\&C_{mnq}^{e}(\theta_k)\frac{j_n\left(k_qr\right)}{r}\Big)\Big]_{r=a}P_{n'}^{m}(\cos\theta_k)\,k_q^2\sin\theta_k d\theta_k.\end{aligned}$$

Optics EXPRESS

From Eq. (10) it can be seen that only the coefficients $G_{mn'q}$ with $m = \pm 1$ have non-trivial solutions. As such, we can represent Eq. (10) as two systems of linear equations (for $m = \pm 1$) in square matrix form with dimensions $2n_{max} \times 2n_{max}$, where n_{max} is the maximum number of n' used in Eqs. (10). The matrices have to be inverted in order to find the unknowns $G_{mn'q}$.

$$\begin{bmatrix} Q^{n\prime}_{mn1} & Q^{n\prime}_{mn2} \\ R^{n\prime}_{mn1} & R^{n\prime}_{mn2} \end{bmatrix} \begin{pmatrix} G_{mn'1} \\ G_{mn'2} \end{pmatrix} = \frac{iE_0}{2\pi (k_0 a)^2} \begin{pmatrix} a^p_{mn} \\ b^p_{mn} \end{pmatrix}. \tag{11}$$

We can now find the coefficients of the scattered fields

$$\begin{aligned} A^s_{mn} =& \frac{1}{h^{(1)}_n (k_0 a)} \Bigg[\frac{1}{E_0} \sum_{q=1}^{2} \sum_{n'=0}^{\infty} 2\pi G_{mn'q} \int_0^{\pi} A^e_{mnq} (\theta_k) \times \\ & j_n \left(k_q a\right) P^m_{n'} (\cos\theta_k) k_q^2 \sin\theta_k d\theta_k - a^p_{mn} j_n (k_0 a) \Bigg], \\ B^s_{mn} =& \frac{1}{h^{(1)}_n (k_0 a)} \Bigg[\frac{i\omega\mu_0}{k_0 E_0} \sum_{q=1}^{2} \sum_{n'=0}^{\infty} 2\pi G_{mn'q} \int_0^{\pi} A^h_{mnq} (\theta_k) \times \\ & j_n \left(k_q a\right) P^m_{n'} (\cos\theta_k) k_q^2 \sin\theta_k \, d\theta_k - b^p_{mn} j_n (k_0 a) \Bigg]. \end{aligned} \tag{12}$$

It is sufficient to calculate the coefficients of the fields scattered by an x-polarized incident beam in order to find the scattering coefficients of y-polarized and circularly polarized incident beams. From Eqs. (6), (7), (10) and (12) we can reach the following relations

$$\begin{aligned} A^s_{1n}|^y &= -iA^s_{1n}|^x, \\ B^s_{1n}|^y &= -iB^s_{1n}|^x, \\ A^s_{-1n}|^y &= iA^s_{-1n}|^x, \\ B^s_{-1n}|^y &= iB^s_{-1n}|^x, \\ A^s_{1n}|^{LCP} &= 2A^s_{1n}|^x, \\ B^s_{1n}|^{LCP} &= 2B^s_{1n}|^x, \\ A^s_{-1n}|^{LCP} &= B^s_{-1n}|^{LCP} = 0, \\ A^s_{1n}|^{RCP} &= B^s_{1n}|^{RCP} = 0, \\ A^s_{-1n}|^{RCP} &= 2A^s_{-1n}|^x, \\ B^s_{-1n}|^{RCP} &= 2B^s_{-1n}|^x, \end{aligned} \tag{13}$$

where the electric field of a RCP incident beam is $\mathbf{E}_{inc} = E_0 (\hat{x} - i\hat{y}) e^{i(kz-\omega t)}$ and the electric field of a LCP incident beam is $\mathbf{E}_{inc} = E_0 (\hat{x} + i\hat{y}) e^{i(kz-\omega t)}$. Similarly, the coefficients of the fields scattered by a beam propagating in the $-z$ direction can be found from the coefficients of the fields scattered by a beam propagating in the $+z$ direction

$$\begin{aligned} A^s_{\pm 1n}|_{-z} &= (-1)^n A^s_{\pm 1n}|_{+z}, \\ B^s_{\pm 1n}|_{-z} &= (-1)^{n+1} B^s_{\pm 1n}|_{+z}. \end{aligned} \tag{14}$$

The fields scattered by a magneto-optical spherical particle conserve the polarization of the incident beam which is nicely demonstrated in Eqs. (6) and 13. For a LCP incident beam, only the coefficients with $m = 1$ are non-zero and as such only scattering coefficients with $m = 1$ have non-trivial solutions. For RCP incident beam, only those with $m = -1$ are non-zero. For clarity, from now on we will refer to $A^s_{mn}|^x_{+z}$ and $B^s_{mn}|^x_{+z}$ as A^s_{mn} and B^s_{mn} respectively.

Optics EXPRESS

3. Scattering and extinction cross sections for magneto-optical particles

We define the scattering cross section as $C_{sca} = \frac{W_s}{I_i}$ [32] where $I_i = \frac{\epsilon_0 c |E_0|^2}{2}$ is the incident irradiance and

$$W_s = \frac{1}{2}\mathrm{Re}\left[\int_0^{2\pi}\int_0^{\pi}\left(E_{s\theta}H^*_{s\phi} - E_{s\phi}H^*_{s\theta}\right) r^2 \sin\theta d\theta d\phi\right], \tag{15}$$

is the rate at which energy is scattered across the surface of an imaginary sphere with arbitrary radius $r \geq a$. $E_{s\theta}$ and $H_{s\theta}$ are the angular components of the scattered fields, $E_{s\phi}$ and $H_{s\phi}$ are the azimuthal components of these fields and H^* is the complex conjugate of H.

The extinction cross section is defined as $C_{ext} = \frac{W_{ext}}{I_i}$ where

$$W_{ext} = \frac{1}{2}\mathrm{Re}\left[\int_0^{2\pi}\int_0^{\pi}\left(E_{i\phi}H^*_{s\theta} - E_{i\theta}H^*_{s\phi} - E_{s\theta}H^*_{i\phi} + E_{s\phi}H^*_{i\theta}\right) r^2 \sin\theta d\theta d\phi\right], \tag{16}$$

is the rate at which energy is extinguished across the surface of the imaginary sphere. Following the same procedure as in Ref. [32], we reach the expression for the scattering cross section

$$C_{sca} = \frac{4\pi}{k_0^2}\sum_n \frac{1}{2n+1}\left[n^2(n+1)^2\left(\left|A^s_{1n}\right|^2 + \left|B^s_{1n}\right|^2\right) + \left|A^s_{-1n}\right|^2 + \left|B^s_{-1n}\right|^2\right]. \tag{17}$$

When the particle is isotropic, $A^s_{-1n} = n(n+1)A^s_{1n}$ and $B^s_{-1n} = -n(n+1)B^s_{1n}$, and so we recover the known expression for scattering cross section with Mie coefficients [32]. The scattering cross section expression is valid for any polarization or direction of the incident beam, as long as the scattering coefficients A^s_{mn} and B^s_{mn} were calculated for that polarization and direction. However, as seen previously, the scattering cross section for circularly polarized incident beam can be calculated from the scattering coefficients of an x-polarized incident beam as follows,

$$\begin{aligned} C^{LCP}_{sca} &= \frac{8\pi}{k_0^2}\sum_n \frac{n^2(n+1)^2}{2n+1}\left(\left|A^s_{1n}\right|^2 + \left|B^s_{1n}\right|^2\right), \\ C^{RCP}_{sca} &= \frac{8\pi}{k_0^2}\sum_n \frac{1}{2n+1}\left(\left|A^s_{-1n}\right|^2 + \left|B^s_{-1n}\right|^2\right). \end{aligned} \tag{18}$$

It can be seen that the scattering cross section of linearly-polarized incident beam is the average of the scattering cross sections of RCP and LCP incident beams. Similarly, we obtain the following expression for the extinction cross section

$$C_{ext} = -\frac{2\pi}{k_0^2}\sum_n \mathrm{Re}\left((-i)^{n+1}\left(n(n+1)(A^s_{1n} + B^s_{1n}) + A^s_{-1n} - B^s_{-1n}\right)\right). \tag{19}$$

When the incident beam is circularly polarized, the extinction cross section can be written as

$$\begin{aligned} C^{LCP}_{ext} &= -\frac{4\pi}{k_0^2}\sum_n \mathrm{Re}\left((-i)^{n+1}n(n+1)(A^s_{1n} + B^s_{1n})\right), \\ C^{RCP}_{ext} &= -\frac{4\pi}{k_0^2}\sum_n \mathrm{Re}\left((-i)^{n+1}\left(A^s_{-1n} - B^s_{-1n}\right)\right). \end{aligned} \tag{20}$$

Up till here, we have presented the necessary theoretical formulation of the electromagnetic fields of a plane wave scattered by a MO sphere. To gain more physical insight into the problem, we will provide in this section some numerical solutions to the problem. As an example for magneto-optical material we use n-doped InSb, a polar semiconductor, that when subjected to an

Optics EXPRESS

external magnetic field becomes magneto-optical [33]. The dielectric permittivity tensor can be considered as a Drude-like metal which, at lowest order in the magnetic field, is given by [33]

$$\begin{aligned}\epsilon_1 =&\epsilon_\infty\left(1+\frac{\omega_L^2-\omega_T^2}{\omega_T^2-\omega^2-i\Gamma_p\omega}+\frac{\omega_p^2(\omega+i\Gamma_f)}{\omega(\omega_c^2-(\omega+i\Gamma_f)^2)}\right),\\ \epsilon_2 =&\frac{i\epsilon_\infty\omega_p^2\omega_c}{\omega[(\omega+i\Gamma_f)^2-\omega_c^2]},\\ \epsilon_3 =&\epsilon_\infty\left(1+\frac{\omega_L^2-\omega_T^2}{\omega_T^2-\omega^2-i\Gamma_p\omega}-\frac{\omega_p^2}{\omega(\omega+i\Gamma_f)}\right).\end{aligned} \tag{21}$$

Here, ϵ_∞ is the high-frequency dielectric constant, ω_L is the longitudinal optical phonon frequency, ω_T is the transverse optical phonon frequency, $\omega_p^2 = n_p e^2/(m^*\epsilon_0\epsilon_\infty)$ is the plasma frequency of free carriers of density n_p and effective mass m^*, Γ_p is the phonon damping constant, and Γ_f is the free carrier damping constant. In all the calculations below, we consider the particular case taken from Ref. [34], where $\epsilon_\infty = 15.7$, $\omega_L = 36.2\times10^{12}$ Hz, $\omega_T = 33.9\times10^{12}$ Hz, $\omega_p = 31.4\times10^{12}$ Hz, $\Gamma_p = 0.565\times10^{12}$ Hz, $\Gamma_f = 3.39\times10^{12}$ Hz, and $m^* = 0.022m_e$. In all the following examples we use n-doped InSb particle of 10μm radius.

In Fig. 2 we plot the evolution of the scattering efficiency (C_{sca}/a^2) as the value of the external magnetic field is increased, for linearly and circularly polarized incident beams.

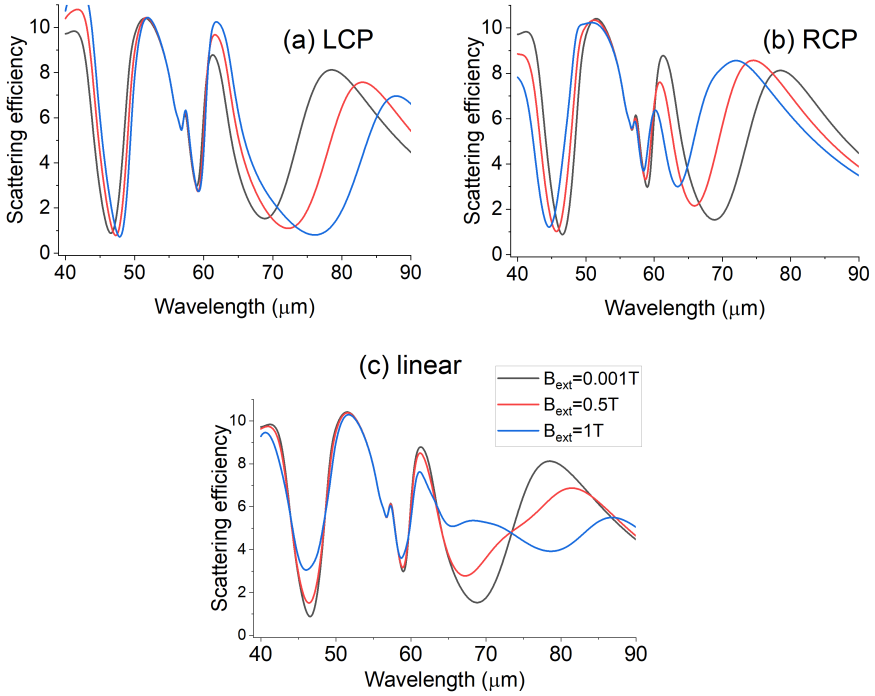

Fig. 2. Scattering efficiency of 10μm radius InSb particle for various values of external magnetic field and for (a) LCP, (b) RCP and (c) linearly polarized incident beams.

It can be seen that for an isotropic particle ($B_{ext} = 0.001T$), the scattering efficiency is independent of the polarization but the circular dichroism in MO scattering changes that.

Note how the scattering efficiency of linearly polarized incident beam is the average of the scattering efficiency of RCP and LCP incident beams and for certain wavelengths (for example

Optics EXPRESS

$\lambda = 76\mu m$ with $B_{ext} = 1T$) the particle is nearly transparent to one helicity and responsive to the other. This resembles the proposed mechanism of maximally chiral particles with dual response [35], but easily tuned with an external magnetic field bias.

In Fig. 3 we plot the contributions to the scattering efficiency from the scattering coefficients of the magnetic and electric dipoles ($A^s_{\pm 11}$ and $B^s_{\pm 11}$) and quadrupoles ($A^s_{\pm 12}$ and $B^s_{\pm 12}$). We plot the contributions for both an isotropic and a magneto-optical particle, where the incident beam is x-polarized.

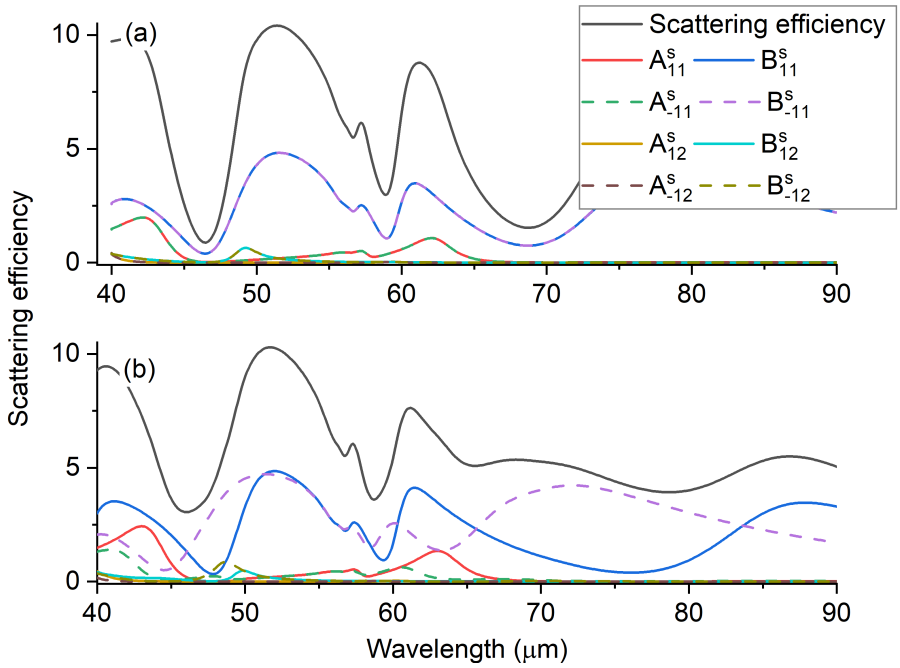

Fig. 3. Contribution to scattering efficiency (for x-polarized incident beam) from scattering coefficients of the magnetic and electric dipoles ($A^s_{\pm 11}$ and $B^s_{\pm 11}$) and quadrupoles ($A^s_{\pm 12}$ and $B^s_{\pm 12}$) for InSb particle of radius $10\mu m$ when (a) $B_{ext} = 0$ and when (b) $B_{ext} = 1T$. In the isotropic case ($B_{ext} = 0$), the contributions of coefficients with $m = 1$ and $m = -1$ are the same. While for the anisotropic case, the contributions are different due to scattering circular dichroism.

In the isotropic case, the contributions to the scattering from coefficients with $m = 1$ (LCP) are the same as the contributions from coefficients with $m = -1$ (RCP). However when an external magnetic field is applied, the cases decouple and the contributions are different.

4. Scattering and extinction cross sections – with the dipole approximation

For comparison, we briefly derive here the expressions for the scattering and extinction cross sections within the dipole approximation for a magneto-optical particle in free space. When an external magnetic field is applied in the z-direction, the particle's polarizability takes a tensor form

$$\hat{\alpha} = \begin{pmatrix} \alpha_{xx} & -\alpha_{xy} & 0 \\ \alpha_{xy} & \alpha_{xx} & 0 \\ 0 & 0 & \alpha_{zz} \end{pmatrix}, \tag{22}$$

Optics EXPRESS

where the derivation of $\hat{\alpha}$ can be found in [17]. From Eqs. (17), 33 and 36, α_{xx} and α_{xy} can be expressed in terms of the scattering coefficients $B^s_{\pm 1n}$ as follows

$$\begin{aligned}\alpha_{xx} &= \frac{2\pi}{k_0^3}\left(2iB^s_{11} - iB^s_{-11}\right),\\ \alpha_{xy} &= -\frac{2\pi}{k_0^3}\left(2B^s_{11} + B^s_{-11}\right).\end{aligned} \tag{23}$$

We define the scattering cross section as [32]

$$C^{dipole}_{sca} = \int_0^{2\pi}\int_0^{\pi} \frac{|\mathbf{T}|^2}{k^2\,|E_i|^2}\sin\theta d\theta d\phi, \tag{24}$$

where $\mathbf{T} = \frac{ik^3}{4\pi\epsilon_m}\hat{r}\times(\hat{r}\times\mathbf{p})$ is the vector scattering amplitude, $\mathbf{p} = \epsilon_0\hat{\alpha}\mathbf{E}$ is the polarization and $|E_i|^2$ is the amplitude of the incident field. After converting the polarization $\mathbf{p}$ to spherical coordinates and integrating with respect to θ and ϕ, we reach the expression for the scattering cross section

$$C^{dipole}_{sca} = \frac{k^4}{6\pi}\left(\left(|\alpha_{xx}|^2 + |\alpha_{xy}|^2\right)\left(|A_{0y}|^2 + |A_{0x}|^2\right) - 4\mathrm{Im}\left(\alpha^*_{xx}\alpha_{xy}\right)\mathrm{Im}\left(A_{0x}A^*_{0y}\right)\right). \tag{25}$$

Similarly, defining the extinction cross section as $C^{dipole}_{ext} = \frac{4\pi}{k^2|E_i|^2}\mathrm{Re}(\mathbf{E}^*_i\cdot\mathbf{T}_{\theta=0})$ [32], we reach the expression

$$C^{dipole}_{ext} = k(\mathrm{Im}(\alpha_{xx})(|A_{0x}|^2 + |A_{0y}|^2) + 2\mathrm{Re}(\alpha_{xy})\mathrm{Im}(A_{0x}A^*_{0y})). \tag{26}$$

The expressions for the extinction and scattering cross sections are the same as obtained by the extended DDA method [36].

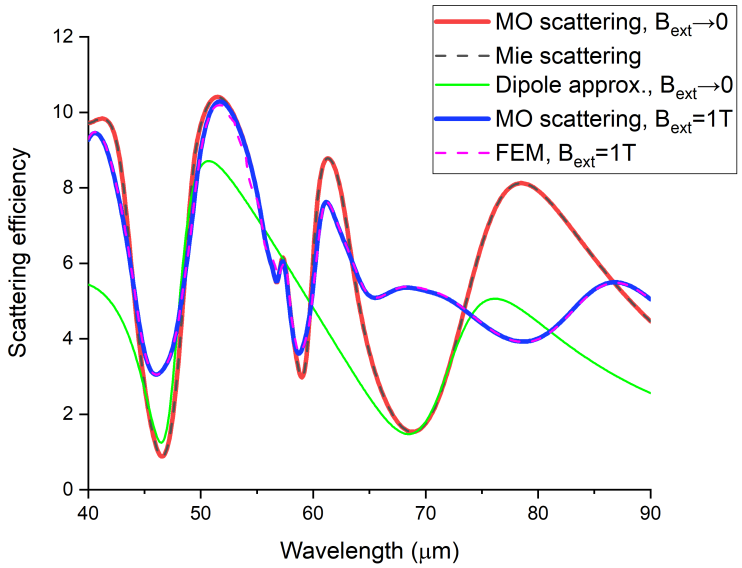

Fig. 4. Scattering efficiency for InSb particle of $10\mu m$ radius. At the limit $B_{ext} \to 0$, both Mie scattering and the method used in this paper (MO scattering) give the same results. When $B_{ext} = 1T$, MO scattering results agree with results from Finite Element Method (FEM).

Optics EXPRESS

In Fig. 4, we plot the scattering efficiency for n-doped InSb particle of $10\mu m$ radius. We calculated the scattering efficiency using three methods, MO scattering with the method used in this paper (Eq. (17)), Mie scattering [32] and the dipole approximation (Eq. (25)). The external magnetic field was set to 0.001T such that the particle is nearly isotropic. It can be seen from Fig. 4 that when the external magnetic field is very small, Mie scattering and magneto-optical scattering are in very good agreement. To further prove the validity of our method, we plot the scattering efficiency for the same particle with an applied external magnetic field of 1T and we compare our results with the Finite Element Method.

5. Optical forces on a magneto-optical particle

For a harmonic electromagnetic field, the time-averaged electromagnetic force on a dielectric particle in a vacuum is given by

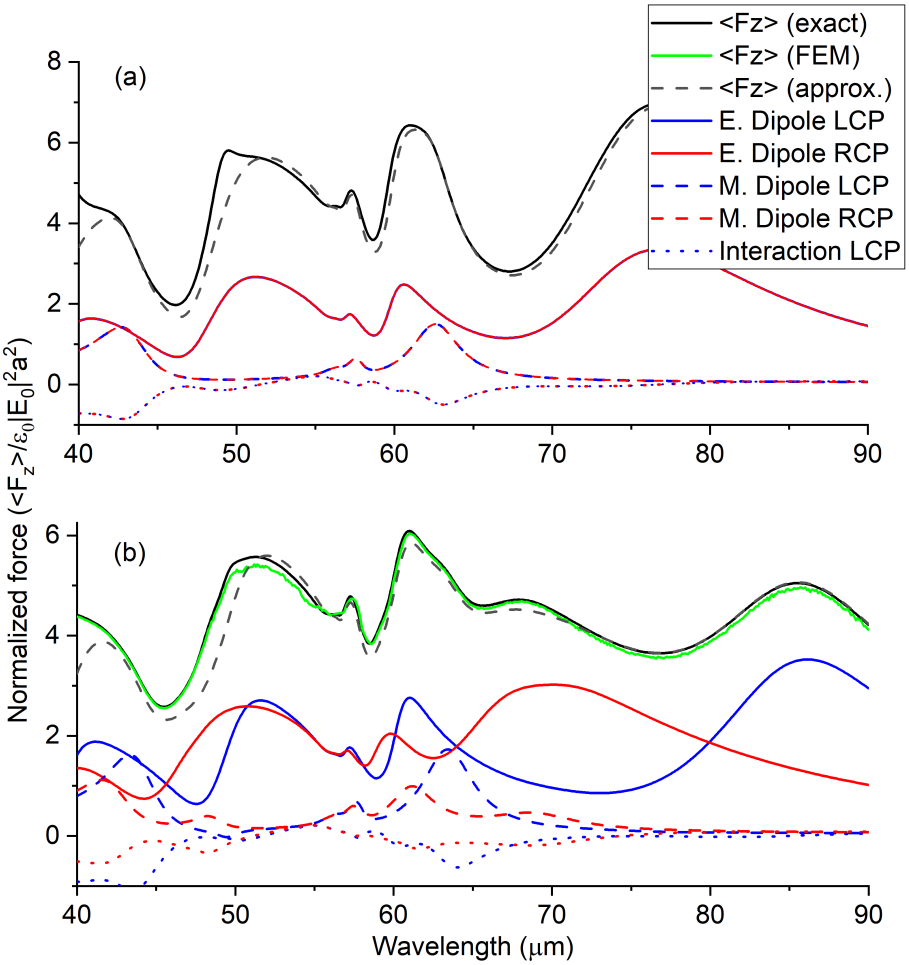

Fig. 5. Normalized force along $\hat{z}$ generated by an x-polarized incident beam on an InSb particle with radius $10\mu m$ when external magnetic field of (a) B_{ext}=0 and (b) B_{ext}=1T is applied. Green line shows the force calculated with the Finite Element Method. Continuous blue and red lines show the contribution to the force from the electric dipole, dashed lines show the contribution from the magnetic dipoles and dotted lines show the contributions from the interactions between the two. For LCP (blue) and RCP (red) polarizations.

Optics EXPRESS

$$\langle \mathbf{F} \rangle = \oint dS \cdot \langle \mathcal{T} \rangle, \tag{27}$$

where the angle brackets stand for the time average, $\mathcal{T}$ is Maxwell's stress tensor in spherical coordinates, and the integral is taken over any surface enclosing the particle where the direction of dS is $\hat{r}$. The expression for the optical force is hence

$$\langle \mathbf{F} \rangle = \frac{1}{2}\mathrm{Re} \oint \left[(\epsilon_0 \mathbf{E}\mathbf{E}^* + \mu_0 \mathbf{H}\mathbf{H}^*) \cdot \hat{r} - \frac{1}{2}((\epsilon_0 \mathbf{E}\cdot\mathbf{E}^* + \mu_0 \mathbf{H}\cdot\mathbf{H}^*)\hat{r}) \right] dS, \tag{28}$$

where the fields $\mathbf{E}$ and $\mathbf{H}$ are the sum of the scattered and the incident fields. The force is composed of cross-interactions between the incident and scattered multipoles $\langle \mathbf{F} \rangle_{is}$ and interactions between different multipoles of different order and degree of the scattered field $\langle \mathbf{F} \rangle_{ss}$. There is no force from the unperturbed incident field since it does not leave any momentum to the scatterer [37].

The Cartesian component of the optical force along the $\hat{z}$ direction $\langle F_z \rangle$ can be expressed in terms of the scattering coefficients and the incident field coefficients [15]. Using the following relations between the spherical wave vectors

$$\begin{aligned} \mathbf{M}^{(l)}_{-1n} &= -\frac{1}{n(n+1)}\mathbf{M}^{(l)*}_{1n}, \\ \mathbf{N}^{(l)}_{-1n} &= -\frac{1}{n(n+1)}\mathbf{N}^{(l)*}_{1n}, \end{aligned} \tag{29}$$

we can adapt the expressions in Ref. [15] to the MO case. As such the force exerted on a magneto-optical particle by a linearly polarized beam is equal to $\langle F_z \rangle_{is} + \langle F_z \rangle_{ss}$ where

$$\begin{aligned} \langle F_z \rangle_{is} =& \frac{\pi\epsilon_0|E_0|^2}{k_0^2}\sum_{n=1}^{\infty}\left[\frac{2n^2(n+1)(n+2)^2}{(2n+1)(2n+3)}\right. \\ & \mathrm{Im}\left(a^x_{1n}(A^{s*}_{1(n+1)} + B^{s*}_{1(n+1)}) + a^{x*}_{1(n+1)}(A^s_{1n} + B^s_{1n})\right) \\ & - \frac{2n(n+1)}{2n+1}\mathrm{Re}\left(a^x_{1n}(A^{s*}_{1n} + B^{s*}_{1n})\right) \\ & + \frac{2n(n+2)}{(n+1)(2n+1)(2n+3)}\mathrm{Im}\left(a^x_{-1n}(A^{s*}_{-1(n+1)} - B^{s*}_{-1(n+1)}) + a^{x*}_{-1(n+1)}(A^s_{-1n} - B^s_{-1n})\right) \\ & \left. - \frac{2}{n(n+1)(2n+1)}\mathrm{Re}\left(a^x_{-1n}(A^{s*}_{-1n} - B^{s*}_{-1n})\right)\right], \\ \langle F_z \rangle_{ss} =& \frac{\pi\epsilon_0|E_0|^2}{k_0^2}\sum_{n=1}^{\infty}\left[\frac{4n^2(n+1)(n+2)^2}{(2n+1)(2n+3)}\mathrm{Im}\left(B^s_{1n}B^{s*}_{1(n+1)} + A^s_{1n}A^{s*}_{1(n+1)}\right)\right. \\ & - \frac{4n(n+1)}{2n+1}\mathrm{Re}\left(A^s_{1n}B^{s*}_{1n}\right) + \frac{4n(n+2)}{(n+1)(2n+1)(2n+3)}\mathrm{Im}\left(B^s_{-1n}B^{s*}_{-1(n+1)} + \right. \\ & \left.\left. A^s_{-1n}A^{s*}_{-1(n+1)}\right) + \frac{4}{n(n+1)(2n+1)}\mathrm{Re}\left(A^s_{-1n}B^{s*}_{-1n}\right)\right]. \end{aligned} \tag{30}$$

If the scattered field is described only by dipoles (both electric and magnetic), we reach a simplified expression for the force

$$\langle F_z \rangle \approx \frac{\epsilon_0\pi|E_0|^2}{k_0^2}\mathrm{Re}\left(2A^s_{11} + 2B^s_{11} + A^s_{-11} - B^s_{-11} - \frac{8}{3}A^s_{11}B^{s*}_{11} + \frac{2}{3}A^s_{-11}B^{s*}_{-11}\right). \tag{31}$$

It can be seen that the force is the sum of the radiation pressures for a pure electric and a pure magnetic dipoles (B^s_{11} and A^s_{11} respectively) and an additional contribution from electric-magnetic

Optics EXPRESS

dipolar interaction [23]. This interaction contribution to the radiation pressure could be negative or positive depending on the signs of the electric and magnetic polarizabilities. We can express the force in terms of extinction cross section (Eq. (19))

$$\langle F_z \rangle \approx \epsilon_0 |E_0|^2 C_{ext} - \frac{2\epsilon_0 \pi |E_0|^2}{3k_0^2} \mathrm{Re}(4A_{11}^s B_{11}^{s*} - A_{-11}^s B_{-11}^{s*}). \tag{32}$$

The force exerted by a circularly polarized beams can be calculated from the scattering coefficients of an x-polarized incident beam

$$\begin{aligned} \langle F_z \rangle^{LCP} &\approx \frac{\epsilon_0 \pi |E_0|^2}{k_0^2} \mathrm{Re}\left(8A_{11}^s + 8B_{11}^s - \frac{32}{3} A_{11}^s B_{11}^{s*}\right), \\ \langle F_z \rangle^{RCP} &\approx \frac{\epsilon_0 \pi |E_0|^2}{k_0^2} \mathrm{Re}\left(4A_{-11}^s - 4B_{-11}^s + \frac{8}{3} A_{-11}^s B_{-11}^{s*}\right). \end{aligned} \tag{33}$$

In Fig. 5 we plot the force in the z-direction exerted by an x-polarized incident beam when (a) no external magnetic field is applied and when (b) an external magnetic field of 1T is applied. Theses forces are normalized in the form $\langle F_z \rangle / (\epsilon_0 |E_0|^2 a^2)$, where $|E_0|$ stands for the modulus of the incident field. The exact force was calculated by numerical integration of Eq. (28). We also plot the force calculated with the Finite Element Methods which shows good agreement with the method used in this paper. The approximated force is calculated with Eq. (31). The approximation deviates from the exact result when higher poles are significant (see also Fig. 3). In the isotropic case, the contributions to the force from the electric and magnetic dipoles are the same for RCP and LCP beams.

For a focused incident beam with power of $1W$, the force on the sphere is between $1.06nN$ and $3.18nN$. In comparison, the gravitational force on the same particle is $0.23nN$.

6. Force on a magneto-optical particle by non-interfering standing waves

A standing wave does not exert any radiation pressure on an isotropic particle. However, it does exert force on a magneto-optical particle [17]. When the incident electromagnetic field is a standing wave which consists of two circularly polarized counter-propagating beams with the same helicity, i.e. $\mathbf{E}_{inc} = E_0 e^{-i\omega t}((e^{ikz} + e^{-ikz})\hat{x} + (ie^{ikz} - ie^{-ikz})\hat{y})$, there is a MO extinction force on the particle [17]. From Eq. (30) and using the relations in Eqs. (13) and 14 we reach an approximated expression for the MO extinction force

$$\langle F_z \rangle_{ext}^{MO} \approx \frac{2\epsilon_0 \pi |E_0|^2}{k_0^2} \mathrm{Re}(4A_{11}^s + 4B_{11}^s - 2A_{-11}^s + 2B_{-11}^s - \frac{16}{3} A_{11}^s B_{11}^{s*} - \frac{4}{3} A_{-11}^s B_{-11}^{s*}). \tag{34}$$

It can be seen that the MO extinction force equals to the difference between the force induced by a LCP beam and the force induced by a RCP beam, when both beams are propagating in the same direction. The MO extinction force is proportional to the extinction circular dichroism (also called the Faraday rotation angle [5]).

$$\langle F_z \rangle_{ext}^{MO} \approx \frac{\epsilon_0 |E_0|^2}{2} (C_{ext}^{LCP} - C_{ext}^{RCP}) - \frac{8\epsilon_0 \pi |E_0|^2}{3k_0^2} \mathrm{Re}(4A_{11}^s B_{11}^{s*} + A_{-1n}^s B_{-1n}^{s*}). \tag{35}$$

When the incident field is a standing wave which consists of two cross polarized counter propagating beams (i.e. an x-polarized beam propagating in the $+z$ direction and a y-polarized beam propagating in the $-z$ direction with total electric field of $\mathbf{E}_{inc} = E_0 e^{-i\omega t}(e^{ikz}\hat{x} + e^{-ikz}\hat{y})$),

Optics EXPRESS

there is a MO gradient force exerted on the particle [17]

$$\langle F_z\rangle_{grad}^{MO} \approx \frac{2\pi\epsilon_0|E_0|^2}{k_0^2}\mathrm{Im}\Big(-2A_{11}^s + 2B_{11}^s + A_{-11}^s + B_{-11}^s + \frac{8}{3}A_{11}^s B_{11}^{s*} + \frac{2}{3}A_{-11}^s B_{-11}^{s*}\Big)\cos(2k_0 z). \tag{36}$$

For an isotropic particle $A_{-11}^s = 2A_{11}^s$ and $B_{-11}^s = -2B_{11}^s$; and so, in the absence of circular dichroism $\langle F_z\rangle_{ext}^{MO} = 0$ and $\langle F_z\rangle_{grad}^{MO} = 0$, as expected. In Fig. 6 we plot the magneto-optical extinction force generated by two circularly polarized incident beams with the same helicity, propagating in opposite directions. In its peak (when incident wavelength is $70\mu m$) and when using focused incident beam with power of $1W$, the magnitude of this force is about 20 times stronger than the gravitational force on the same particle.

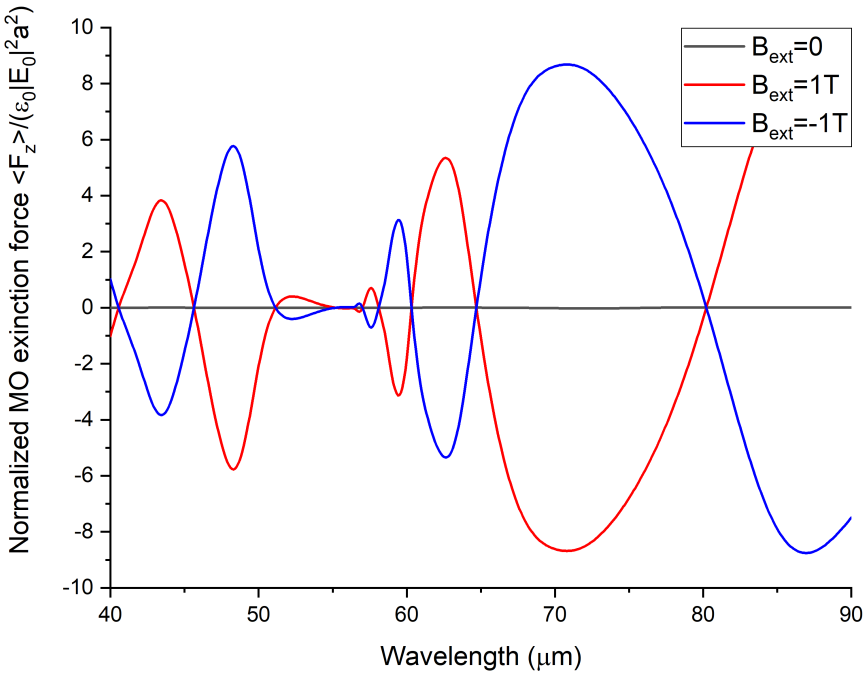

Fig. 6. Magneto-optical extinction force on a n-doped InSb particle of $10\mu m$ radius for various external magnetic field values.

In Fig. 7 we plot the differential scattering cross section for the same particle when the wavelength is $48\mu m$. As can be seen in Fig. 6, at this wavelength, the force is positive when the external magnetic field is negative and vice versa. Figure 7 demonstrates that the MO extinction force is due to directional scattering. When the force is positive (Fig. 7(b)) there is no forward scattering (we take forward to be in the $+z$ direction) and when the force is negative (Fig. 7(c)) there is no backward scattering.

Note how the scattered field is almost completely circularly polarized even though the incident field has an undefined spin.

Optics EXPRESS

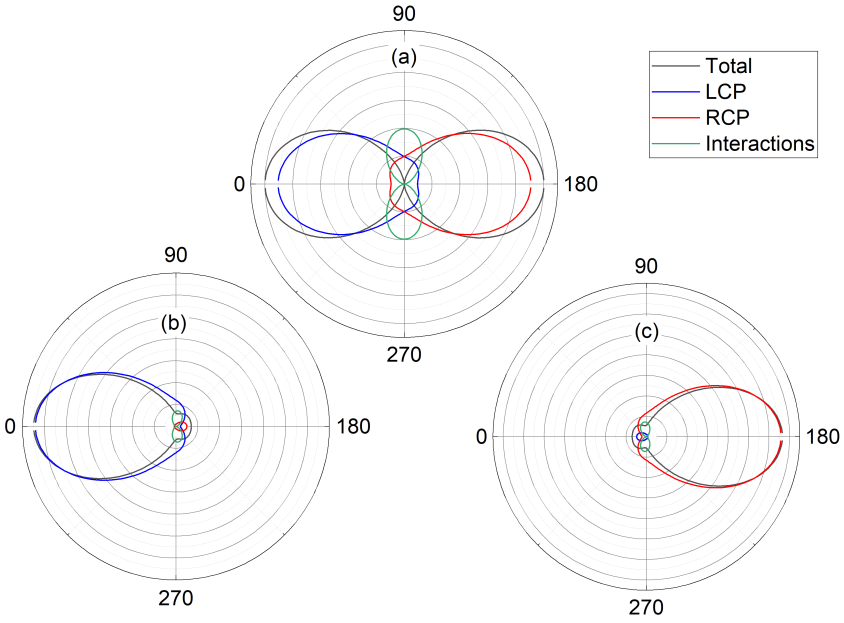

Fig. 7. Differential scattering cross section $(dCsca(\theta)/d\Omega)$ for a InSb particle in an incident field composed of two counter propagating circularly polarized beams with the same helicity. Black line represents the total field, blue line represents the contribution from LCP field, red line the contribution from RCP field and green line the contribution from interaction between RCP and LCP. (a) $B_{ext} = 0$, no MO extinction force. (b) $B_{ext} = -1T$, MO extinction force in the $+z$ direction and (c) $B_{ext} = 1T$, MO extinction force in the $-z$ direction. The particle is of $10\mu m$ radius and the wavelength of the incident beams is $48\mu m$.

7. Numerical methods

The computation of the scattered field coefficients was carried out by two steps. In the first step, the matrix elements in Eq. (11) were evaluated using numerical integration. In the second step the linear equations were solved by computing the inverse of the matrix.

We used built in functions of the software Mathematica for the calculation of the spherical Bessel and Hankel functions and for the associated Legendre functions. The numerical integration was performed using an adaptive strategy which reaches the required precision and accuracy goals of the integral by recursive bisection of the sub-region with the largest error estimate into two halves and computes integral and error estimates for each half (see Mathematica manual for more details, https://reference.wolfram.com/language/tutorial/NIntegrateIntegrationStrategies.html). To speed-up the integration we used parallel computing, evaluating the integrals for the matrix cells in parallel. The method for finding the solutions for the linear equations is automatically chosen by the software Mathematica (for more information see manual https://reference.wolfram.com/language/ref/LinearSolve.html).

8. Conclusions

By expansion of the scattered and incident fields with spherical vector wave functions, and Fourier transform of the internal fields, we could use boundary conditions to resolve the scattering of plane wave by a magneto-optical sphere.

We have derived expressions for the scattering and extinction cross sections as well as for the forces exerted on a magneto-optical particle, expressed in terms of the scattering coefficients. We showed that when the external magnetic field is zero, those expressions coincide with the

Optics EXPRESS

known expressions that use Mie scattering coefficients for isotropic particles. The method we used helps understand intuitively the circular dichroism in magneto-optical scattering and forces.

In the numerical calculations, we showed that the magneto-optical extinction force results from directional scattering. This radiation forces, based on the magneto-optical effect, might open routes to applications in the fields of optical manipulation, sensors, and enhancement of circular dichroism spectroscopy.

A. Coefficients of internal field

Following are the expressions for the coefficients $A^{e,h}_{\pm 1nq}$, $B^{e,h}_{\pm 1nq}$ and $C^{e,h}_{\pm 1nq}$ which are used in Eqs. (9)–(12). Their derivation can be found in Ref. [19].

$$A^{e,h}_{1nq} = A^{e1,h1}_{1nq} + A^{e2,h2}_{1nq} \tag{37}$$

$$B^{e,h}_{1nq} = B^{e1,h1}_{1nq} + B^{e2,h2}_{1nq} \tag{38}$$

$$C^{e,h}_{1nq} = C^{e1,h1}_{1nq} + C^{e2,h2}_{1nq} \tag{39}$$

where

$$\begin{aligned}
A^{e1}_{1nq} =& i^n \frac{2n+1}{2n^2(n+1)^2}\frac{\Delta_1}{\Delta}\left(n(n+1)P^0_n - P^2_n\right),\\
A^{e2}_{1nq} =& i^{n+1}\frac{2n+1}{2n^2(n+1)^2}\Big[\frac{\Delta_2}{\Delta}\left(n(n+1)P^0_n + P^2_n\right) + 2P^1_n\Big],\\
B^{e1}_{1nq} =& \frac{i^n}{2n^2(n+1)^2}\frac{\Delta_1}{\Delta}\left[n(n+1)^2P^0_{n-1} + (n+1)P^2_{n-1} + n^2(n+1)P^0_{n+1} + nP^2_{n+1}\right],\\
B^{e2}_{1nq} =& \frac{i^n}{2n^2(n+1)^2}\Big[\frac{i\Delta_2}{\Delta}(n(n+1)^2P^0_{n-1} - (n+1)P^2_{n-1} + n^2(n+1)P^0_{n+1} - nP^2_{n+1}\Big]\\
&+ 2n^2iP^1_{n+1} - 2(n+1)^2iP^1_{n-1}),\\
C^{e1}_{1nq} =& \frac{i^n}{2k_qn(n+1)}\frac{\Delta_1}{\Delta}\left[n(n+1)P^0_{n-1} + P^2_{n-1} - n(n+1)P^0_{n+1} - P^2_{n+1}\right],\\
C^{e2}_{1nq} =& \frac{i^n}{k_q2n(n+1)}\Big[\frac{i\Delta_2}{\Delta}(n(n+1)P^0_{n-1} - P^2_{n-1} - n(n+1)P^0_{n+1} + P^2_{n+1})\\
&- 2(2n+1)\cos\theta_k iP^1_n\Big],\\
A^{h1}_{1nq} =& i^{n+1}\frac{k_q}{\omega\mu_0}\frac{2n+1}{2n^2(n+1)^2}\Big[-\cos\theta_k\frac{\Delta_1}{\Delta}(n(n+1)P^0_n + P^2_n) + 2P^1_n\sin\theta_k\Big],\\
A^{h2}_{1nq} =& i^{n+1}\frac{k_q}{\omega\mu_0}\frac{2n+1}{2n^2(n+1)^2}\Big[-\cos\theta_k\frac{i\Delta_2}{\Delta} + i\sin\theta_k)(n(n+1)P^0_n - P^2_n\Big],
\end{aligned} \tag{40}$$

$$\begin{aligned}
B^{h1}_{1nq} =& \frac{k_q}{\omega\mu_0}\frac{i^{n+1}}{2n^2(n+1)^2}\frac{\Delta_1}{\Delta}\Big[-\cos\theta_k\left(n(n+1)^2P^0_{n-1} - (n+1)P^2_{n-1} + n^2(n+1)P^0_{n+1}\right.\\
&\left.- nP^2_{n+1}\right) + 2\sin\theta_k\left(n^2P^1_{n+1} - (n+1)^2P^1_{n-1}\right)\Big],\\
B^{h2}_{1nq} =& \frac{k_q}{\omega\mu_0}\frac{i^{n+1}}{2n^2(n+1)^2}\left(\frac{-i\Delta_2}{\Delta}\cos\theta_k + i\sin\theta_k\right)\left[n(n+1)^2P^0_{n-1} + (n+1)P^2_{n-1}\right.\\
&\left.+ n^2(n+1)P^0_{n+1} + nP^2_{n+1}\right],\\
C^{h1}_{1nq} =& \frac{i^{n+1}}{2\omega\mu_0n(n+1)}\frac{\Delta_1}{\Delta}\Big[-\cos\theta_k(n(n+1)(P^0_{n-1} - P^0_{n+1}) - P^2_{n-1} + P^2_{n+1})\\
&- 2(2n+1)\sin\theta_k\cos\theta_kP^1_n\Big],\\
C^{h2}_{1nq} =& \frac{i^{n+1}}{\omega\mu_02n(n+1)}\left(\frac{-i\Delta_2}{\Delta}\cos\theta_k + i\sin\theta_k\right)\left(n(n+1)(P^0_{n-1} - P^0_{n+1}) + P^2_{n-1} - P^2_{n+1}\right).
\end{aligned}$$

P^m_n is the associated Legendre function with the parameter $\cos(\theta_k)$, $\Delta_1 = a_2k_q^2\sin\theta_k\cos\theta_k$, $\Delta_2 = (k_q^2 - a_1)k_q^2\sin\theta_k\cos\theta_k$ and $\Delta = k_q^4\cos^2\theta_k - a_1k_q^2(1+\cos^2\theta_k) + (a_1^2 + a_2^2)$.

Optics EXPRESS

The coefficients for $m = -1$ can be derived as follows

$$\begin{aligned} A^{e,h}_{-1nq} &= n(n+1)(-A^{e1,h1}_{1nq} + A^{e2,h2}_{1nq}), \\ B^{e,h}_{-1nq} &= n(n+1)(B^{e1,h1}_{1nq} - B^{e2,h2}_{1nq}), \\ C^{e,h}_{-1nq} &= n(n+1)(C^{e1,h1}_{1nq} - C^{e2,h2}_{1nq}). \end{aligned} \tag{41}$$

Funding. Comunidad de Madrid (SI1/PJI/2019-00052); Ministerio de Ciencia e Innovación (CEX2018-000805-M, PGC2018-095777-B-C21, PGC2018-095777-B-C22, PID2019-109905GA-C22).

Disclosures. The authors declare no conflicts of interest.

Data availability. Data and code which were used to generate the results presented in this paper are not publicly available at this time but may be obtained from the authors upon request.

References

1. G. Armelles, A. Cebollada, A. García-Martín, and M. U. González, "Magnetoplasmonics: Combining magnetic and plasmonic functionalities," Adv. Opt. Mater. **1**(1), 10–35 (2013).
2. N. Maccaferri, I. Zubritskaya, I. Razdolski, I. A. Chioar, V. Belotelov, V. Kapaklis, P. M. Oppeneer, and A. Dmitriev, "Nanoscale magnetophotonics," J. Appl. Phys. **127**(8), 080903 (2020).
3. G. W. Ford and S. A. Werner, "Scattering and absorption of electromagnetic waves by a gyrotropic sphere," Phys. Rev. B **18**(12), 6752–6769 (1978).
4. W. Ren, "Contributions to the electromagnetic wave theory of bounded homogeneous anisotropic media," Phys. Rev. E **47**(1), 664–673 (1993).
5. D. A. Smith and K. L. Stokes, "Discrete dipole approximation for magnetooptical scattering calculations," Opt. Express **14**(12), 5746–5754 (2006).
6. N. de Sousa, L. S. Froufe-Pérez, J. J. Sáenz, and A. García-Martín, "Magneto-optical activity in high index dielectric nanoantennas," Sci. Rep. **6**(1), 30803 (2016).
7. Z. Chen, H. Zhang, X. Wu, and Z. Huang, "Gaussian beam scattering by a gyrotropic anisotropic object," J. Quant. Spectrosc. Radiat. Transfer **180**, 1–6 (2016).
8. J. L. W. Li, W. L. Ong, and K. H. R. Zheng, "Anisotropic scattering effects of a gyrotropic sphere characterized using the t-matrix method," Phys. Rev. E **85**(3), 036601 (2012).
9. V. Schmidt and T. Wriedt, "The t-matrix for particle with arbitrary permittivity tensor and parallelization of the computational code," J. Quant. Spectrosc. Radiat. Transfer **113**(13), 1712–1718 (2012).
10. J. J. Wang, Y. P. Han, Z. F. Wu, and L. Han, "T-matrix method for electromagnetic scattering by a general anisotropic particle," J. Quant. Spectrosc. Radiat. Transfer **162**, 66–76 (2015).
11. G. Gouesbet, B. Maheu, and G. Gréhan, "Light scattering from a sphere arbitrarily located in a gaussian beam, using a bromwich formulation," J. Opt. Soc. Am. A **5**(9), 1427–1443 (1988).
12. K. Ren, G. Gréha, and G. Gouesbet, "Radiation pressure forces exerted on a particle arbitrarily located in a gaussian beam by using the generalized lorenz-mie theory, and associated resonance effects," Opt. Commun. **108**(4-6), 343–354 (1994).
13. Y. Harada and T. Asakura, "Radiation forces on a dielectric sphere in the rayleigh scattering regime," Opt. Commun. **124**(5-6), 529–541 (1996).
14. P. C. Chaumet and M. Nieto-Vesperinas, "Time-averaged total force on a dipolar sphere in an electromagnetic field," Opt. Lett. **25**(15), 1065–1067 (2000).
15. A. Salandrino, S. Fardad, and D. N. Christodoulides, "Generalized mie theory of optical forces," J. Opt. Soc. Am. B **29**(4), 855–866 (2012).
16. J. P. Barton, D. R. Alexander, and S. A. Schaub, "Theoretical determination of net radiation force and torque for a spherical particle illuminated by a focused laser beam," J. Appl. Phys. **66**(10), 4594–4602 (1989).
17. S. Edelstein, R. M. Abraham-Ekeroth, P. A. Serena, J. J. Sáenz, A. García-Martín, and M. I. Marqués, "Magneto-optical stern-gerlach forces and nonreciprocal torques on small particles," Phys. Rev. Res. **1**(1), 013005 (2019).
18. S. Edelstein, A. García-Martín, P. A. Serena, and M. I. Marqués, "Magneto-optical binding in the near field," Sci. Rep. **11**(1), 20820 (2021).
19. Y. Geng, X. Wu, and L. W. Li, "Analysis of electromagnetic scattering by a plasma anisotropic sphere," Radio Sci. **38**(6), 1 (2003).
20. A. K. Zvezdin and V. A. Kotov, *Modern Magnetooptics and Magnetooptical Materials* (CRC Press, 1997).
21. B. Han, X. Gao, J. Lv, and Z. Tang, "Magnetic circular dichroism in nanomaterials: New opportunity in understanding and modulation of excitonic and plasmonic resonances," Adv. Mater. **32**(41), 1801491 (2020).
22. M. Nieto-Vesperinas, "Chiral optical fields: a unified formulation of helicity scattered from particles and dichroism enhancement," Philos. Trans. R. Soc., A **375**(2090), 20160314 (2017).
23. M. Nieto-Vesperinas, J. J. Sáenz, R. Gómez-Medina, and L. Chantada, "Optical forces on small magnetodielectric particles," Opt. Express **18**(11), 11428–11443 (2010).

Optics EXPRESS

24. G. Gouesbet, V. D. Angelis, and L. André Ambrosio, "Optical forces and optical force categorizations on small magnetodielectric particles in the framework of generalized lorenz-mie theory," J. Quant. Spectrosc. Radiat. Transfer **279**, 108046 (2022).
25. L. A. Ambrosio, V. S. de Angelis, and G. Gouesbet, "The generalized lorenz-mie theory and its identification with the dipole theory of forces for particles with electric and magnetic properties," J. Quant. Spectrosc. Radiat. Transfer **281**, 108104 (2022).
26. H. T. Chen, A. J. Taylor, and N. Yu, "A review of metasurfaces: physics and applications," Rep. Prog. Phys. **79**(7), 076401 (2016).
27. D. R. Abujetas, N. de Sousa, A. García-Martín, J. M. Llorens, and J. A. Sánchez-Gil, "Active angular tuning and switching of brewster quasi bound states in the continuum in magneto-optic metasurfaces," Nanophotonics **10**(17), 4223–4232 (2021).
28. Q. Mu, F. Fan, S. Chen, S. Xu, C. Xiong, X. Zhang, X. Wang, and S. Chang, "Tunable magneto-optical polarization device for terahertz waves based on insb and its plasmonic structure," Photonics Res. **7**(3), 325–331 (2019).
29. M. Q. Liu, C. Y. Zhao, and B. X. Wang, "Active tuning of directional scattering by combining magneto-optical effects and multipolar interferences," Nanoscale **10**(38), 18282–18290 (2018).
30. J. Lasa-Alonso, D. R. Abujetas, Á. Nodar, J. A. Dionne, J. J. Sáenz, G. Molina-Terriza, J. Aizpurua, and A. García-Etxarri, "Surface-enhanced circular dichroism spectroscopy on periodic dual nanostructures," ACS Photonics **7**(11), 2978–2986 (2020).
31. D. Sarkar and N. J. Halas, "General vector basis function solution of maxwell's equations," Phys. Rev. E **56**(1), 1102–1112 (1997).
32. C. F. Bohren and D. R. Huffman, *Absorption and Scattering of Light by Small Particles* (Wiley, 1983).
33. E. D. Palik, R. Kaplan, R. W. Gammon, H. Kaplan, R. F. Wallis, and J. J. Quinn, "Coupled surface magnetoplasmon-optic-phonon polariton modes on insb," Phys. Rev. B **13**(6), 2497–2506 (1976).
34. E. Moncada-Villa, V. Fernández-Hurtado, F. J. García-Vidal, A. García-Martín, and J. C. Cuevas, "Magnetic field control of near-field radiative heat transfer and the realization of highly tunable hyperbolic thermal emitters," Phys. Rev. B **92**(12), 125418 (2015).
35. A. Rahimzadegan, M. Fruhnert, R. Alaee, I. Fernandez-Corbaton, and C. Rockstuhl, "Optical force and torque on dipolar dual chiral particles," Phys. Rev. B **94**(12), 125123 (2016).
36. R. A. de la Osa, P. Albella, J. M. Saiz, F. González, and F. Moreno, "Extended discrete dipole approximation and its application to bianisotropic media," Opt. Express **18**(23), 23865–23871 (2010).
37. G. Gouesbet, G. Grehan, and B. Maheu, "Scattering of a gaussian beam by a mie scatter center using a bromwich formalism," J. Opt. **16**(2), 83–93 (1985).